

## PAPER

View Article Online  
View Journal | View IssueCite this: *Green Chem.*, 2024, **26**, 11695

# Valorization of pomegranate waste through green solvent extraction and biochar production: a zero-waste biorefinery approach†

Leonardo M. de Souza Mesquita,<sup>a</sup> Letícia S. Contieri,<sup>a,b</sup> Bárbara M. C. Vaz,<sup>b</sup> Vitor Sencadas,<sup>c</sup> Filipe H. B. Sosa,<sup>b</sup> João A. P. Coutinho,<sup>b</sup> Maurício A. Rostagno<sup>a</sup> and Sónia P. M. Ventura<sup>a,b</sup>

This study introduces a sustainable, zero-waste biorefinery approach for the valorization of pomegranate (*Punica granatum*) waste, focusing on the sequential extraction of anthocyanins, ellagic acid and its derivatives using environmentally friendly solvents, followed by biochar production. Initially, a COSMO-RS *in silico* analysis was conducted, screening 10 512 combinations of hydrogen bond acceptors (HBAs) and hydrogen bond donors (HBDs) typically used in eutectic solvent formulations, along with 49 bio-based solvents, to identify the most efficient green solvents for recovering anthocyanins, ellagic acid and its derivatives. In the first step, an aqueous solution of gamma-valerolactone (GVL) (2900 mM, pH 2) was used for solid–liquid extraction; this led to the optimization of extraction conditions (solid–liquid ratio of 0.07 g<sub>biomass</sub> mL<sub>solvent</sub><sup>−1</sup>, at 25 °C for 55 minutes) yielding 38.52 ± 0.06 mg<sub>anthocyanins</sub> g<sub>biomass</sub><sup>−1</sup>. Subsequently, the residual biomass underwent a second extraction using an aqueous solution of the ionic liquid (IL) cholinium acetate (2900 mM, pH 13) under similar conditions, yielding a rich fraction of ellagic acid and its derivatives (21.82 mg<sub>ellagic acid</sub> g<sub>biomass</sub><sup>−1</sup>). The remaining biomass was then converted into activated biochar using a eutectic solvent composed of cholinium chloride and oxalic acid (molar ratio 1 HBA : 2 HBD), providing a greener alternative to traditional biochar production methods. The resulting biochar was utilized as an adsorbent for removing synthetic dyes (food and textile) from aqueous solutions, presenting new opportunities for the remediation of contaminated water effluents. This zero-waste process fully valorizes pomegranate residues, adhering to green extraction principles and achieving a Path2Green score of 0.401 (corresponding to around 288.50 g<sub>CO<sub>2</sub></sub> g<sub>biomass</sub><sup>−1</sup>), underscoring its eco-friendliness. By minimizing waste and reducing the need for harmful organic solvents, this biorefinery model highlights the potential for greener industrial practices through the use of bio-based solvents and the complete utilization of biomass.

Received 26th July 2024,  
Accepted 16th October 2024

DOI: 10.1039/d4gc03707c

rsc.li/greenchem

## Introduction

In the coming years, the global society will face several challenges, many linked to maintaining life standards and the well-being of populations. One of the most worrisome chal-

lenges is the reduction of greenhouse gas emissions and the adaptation of existing technologies to new sustainable alternatives, enabling climate change mitigation while maintaining the supply of resources.<sup>1</sup> Several global meetings have been addressing this problem, and their most relevant conclusions are exposed in the Sustainable Development Goals (SDGs) published in the 2030 agenda of the United Nations,<sup>2</sup> encouraging the scientific community to discover how to protect the planet and ensure that all people enjoy peace and prosperity. In this sense, many interdisciplinary strategies are required to address these challenging tasks. Among them, the circular economy and the biorefinery, which intend to convert biomass into a wide range of products, including biofuels, chemicals, and materials,<sup>3</sup> are expected to provide significant contributions. However, despite their generous goal, biorefinery approaches could generate a high environmental impact if

<sup>a</sup>Multidisciplinary Laboratory of Food and Health (LabMAS), School of Applied Sciences (FCA), University of Campinas, Rua Pedro Zaccaria 1300, 13484-350 Limeira, Sao Paulo, Brazil. E-mail: mesquitals@gmail.com

<sup>b</sup>Department of Chemistry, CICECO – Aveiro Institute of Materials, University of Aveiro Campus Universitário de Santiago, 3810-193 Aveiro, Portugal.

E-mail: spventura@ua.pt

<sup>c</sup>Department of Materials Science and Ceramic Engineering, CICECO – Aveiro Institute of Materials, University of Aveiro Campus Universitário de Santiago, 3810-193 Aveiro, Portugal

† Electronic supplementary information (ESI) available. See DOI: <https://doi.org/10.1039/d4gc03707c>

poorly designed, especially when using non-benign raw materials and high-energy techniques.<sup>4</sup> Thus, to prospect for a real sustainable biorefinery, it is necessary to integrate a circular economy-based concept on safe, economical, and eco-friendly approaches.<sup>5</sup>

Associated with SDGs 12 (sustainable consumption and production) and 13 (climate action), bio-based solvents are excellent candidates for application in new biorefineries since they are considered greener alternatives to fossil fuel-based organic solvents, contributing to more sustainable production systems and, as a result, reducing carbon footprint.<sup>6</sup> A bio-based solvent results from renewable biological sources, such as plants or microorganisms, and can be used in several applications, including for the extraction of bioactive compounds from biomass.<sup>7,8</sup> Another promising class of solvents available for the development of more sustainable biorefinery platforms is known as non-volatile alternative solvents, mainly represented by ionic liquids – ILs – and eutectic mixtures [mostly known as (deep) eutectic solvents – (D)ESs]. ILs are pure substances characterized as molten salts composed of ions of different dimensions. These lead to unique properties like low vapor pressure, high thermal stability, and a wide liquid range.<sup>9</sup>

In contrast, (D)ESs are mixtures of two or more hydrogen bond donors and acceptors, with a significantly lower melting point than any of their starting components.<sup>10</sup> Both ILs and (D)ESs are considered by many scientists as “green solvents”. However, this may not be entirely true, considering that some classes of these solvents have already been demonstrated to be toxic and associated with a high carbon footprint in their synthesis/formation.<sup>11–13</sup> For these reasons, it is essential not to create overgeneralizations regarding the use of these solvents.<sup>14</sup> Indeed, they are alternatives, but it is crucial to design innovative applications that can be used without risk to the user's health and the environment.

Aligned with SDG 2 (Zero Hunger), the valorization of discarded or wasted foods addresses food security by transforming waste into valuable resources. This approach also supports SDG 11 (Sustainable Cities and Communities) by promoting efficient waste management practices in urban settings. By minimizing food waste, we contribute to SDG 13 (Climate Action) by reducing greenhouse gas emissions associated with organic waste decomposition. Furthermore, it supports SDG 14 (Life Below Water) and SDG 15 (Life on Land) by preventing pollution and nutrient runoff that can harm aquatic ecosystems and terrestrial environments. In this sense, about 30% of world food production is wasted, mainly the highly perishable vegetables and fruits.<sup>15</sup> This aspect directly impacts human well-being by increasing social inequality, the volume of garbage in landfills, and pollution of aquatic systems. In the past 20 years, there has been an increase of 40 times in studies concerning food waste, highlighting this issue's importance and how the scientific community has been looking for new alternatives to remediate it. *Punica granatum* (pomegranate) is a worldwide appreciated fruit, especially in India, Iran, Turkey, and the United States.<sup>16</sup> Despite pomegranate being con-

sidered a minor crop, its production has increased in recent years due to the high demand for its juice, considering a healthier alternative to those made from oranges and apples, which have a lower diversity of chemical compounds and consequently lower health benefits. Its intake is associated with several health benefits, from antioxidant to anti-tumor, anti-inflammatory, neuroprotection, anti-viral, and anti-bacterial.<sup>17</sup> However, only a fraction of the pomegranate produced is consumed; with 54% being wasted, mainly in the form of seeds and peels,<sup>18</sup> which establishes the need to repurpose that waste.

Among the major bioactive compounds from pomegranate, phenolics are highlighted, mainly anthocyanins and ellagic acid and derivatives.<sup>19</sup> SDG 3 (Good Health and Well-being) is contemplated by the importance of phenolic compounds in our lives since these compounds are associated with higher life expectations and a lower need for traditional medicines.<sup>20</sup> Anthocyanins are natural reddish-purple pigments commonly present in pomegranate peels. However, despite their intense color, some drawbacks concerning their utilization as dyes need to be overcome, mainly regarding their color stability when submitted to high temperatures and alkaline pH values.<sup>21</sup> Ellagic acid, a bright yellow compound, is a colorant agent and preservative compound for food products. It is also present in high concentrations in pomegranate wastes (mainly due to its poor water solubility). Still, a promising market niche is the cosmetic industry, especially for pharmaceutical and skin care products.<sup>22</sup> Unfortunately, synthetic pigments are still preferred as colorants in food- and cosmetic-based products, leading to health and environmental problems.<sup>23,24</sup> Thus, looking for new alternatives to extract and stabilize natural pigments is a hot topic today, especially considering that synthetic pigments will be banned as food colorants in the European Union by 2030,<sup>25</sup> meeting SDG 12, as it promotes sustainable practices in the production of natural pigments, reduces reliance on harmful synthetic chemicals, and encourages the efficient use of renewable resources.

After all industrial bioprospection processes, residual biomass is still persistent and inevitably must be discarded, consequently generating an environmental impact. Then, based on the recent trends in searching for new and non-expensive adsorbent materials, producing biochar with waste seems to be an excellent alternative to repurposing this material. Initially, it was produced as a soil fertilizer, but other applications have been proposed, such as soil remediation, water treatments, and CO<sub>2</sub> capture.<sup>26–28</sup> Three conventional methods are used to produce biochar, namely, (i) pyrolysis, (ii) hydrothermal carbonization, and (iii) microwave carbonization.<sup>29</sup> However, all these techniques are very high-energy consuming due to the high reaction temperatures required, usually higher than 400 °C. Thus, technological innovations are desired to meet SDG 9 (industry, innovation, and infrastructure) and maximize the environmental benefits of producing biochar materials.

This work proposes developing an efficient biorefinery process mediated by bio-based solvents to recover natural pig-

ments from pomegranate wastes, namely anthocyanins, ellagic acid, and its derivatives. For this purpose, several processual conditions were optimized (Solid–Liquid Ratio – SLR, in  $\text{mg}_{\text{bio-mass}} \text{mL}_{\text{solvent}}^{-1}$ ; concentration of the solvent –  $C$ , in M; pH; and time of extraction –  $t_{\text{ext}}$ , in min). All the biorefinery steps were optimized *via* the design of experiments (DoEs). After optimizing the pigments' recovery, the residual biomass was used to produce biochar by an alternative methodology based on (D)ESs, whose applicability was demonstrated in a simple process of adsorption of synthetic dyes from aqueous solutions (proof of concept). Thus, a closed-loop biorefinery approach was developed in this work, using non-toxic raw materials, respecting sustainability and circular economy concepts.

## Materials and methods

### Biomass – pomegranate

*Punica granatum* (pomegranate waste) cake, after juice production, was obtained from the American industry – Pom Wonderful LLC (Los Angeles, California, USA). The sample was then autoclaved to avoid contamination by microorganisms and enzymes (121 °C, 15 min, 5 bar) and then subjected to knife milling to standardize the particle size (#50 mesh) and freeze-dried to ensure the compound's integrity.

### Chemicals

Acetone, ethanol, and methanol (absolute grade) were purchased from Thermo Fisher Scientific as control solvents for extracting the bioactive compounds from pomegranate wastes. The alternative solvents used in this work were the following: cholinium acetate ( $[\text{Ch}][\text{OAc}]$ , >99%) purchased from Iolitec, and tetraethylammonium chloride ( $[\text{N}_{2,2,2,2}]\text{Cl}$ , 98%) acquired from Alfa Aesar. Betaine (98%), urea (99.5%), methyl urea (97%), and 1,3-dimethylurea (98%) were obtained from Acros Organics. 1,3-Butanediol (99.5%) was purchased from Sigma-Aldrich. Gamma-valerolactone (GVL, 98%), and cyrene (99%) were acquired from Merck. Ethanol absolute (HPLC grade) was obtained for chromatographic analysis from Sigma-Aldrich. The ultra-pure water used in all the solutions was provided by a Purelab Flex 3 purifying system (ElgaVeolia, High Wycombe, UK). The reagents used in the anthocyanins' quantification analysis, namely sodium acetate (100%) and potassium chloride (99.5%), were purchased from Sigma-Aldrich. The (D)ESs used to produce the biochar material after extraction of the target compounds were composed of cholinium chloride –  $[\text{Ch}]\text{Cl}$  (98%, Acros Organics) as HBA and oxalic acid (OA) (Alfa Aesar, 100%) as HBD.

### Screening of solvents

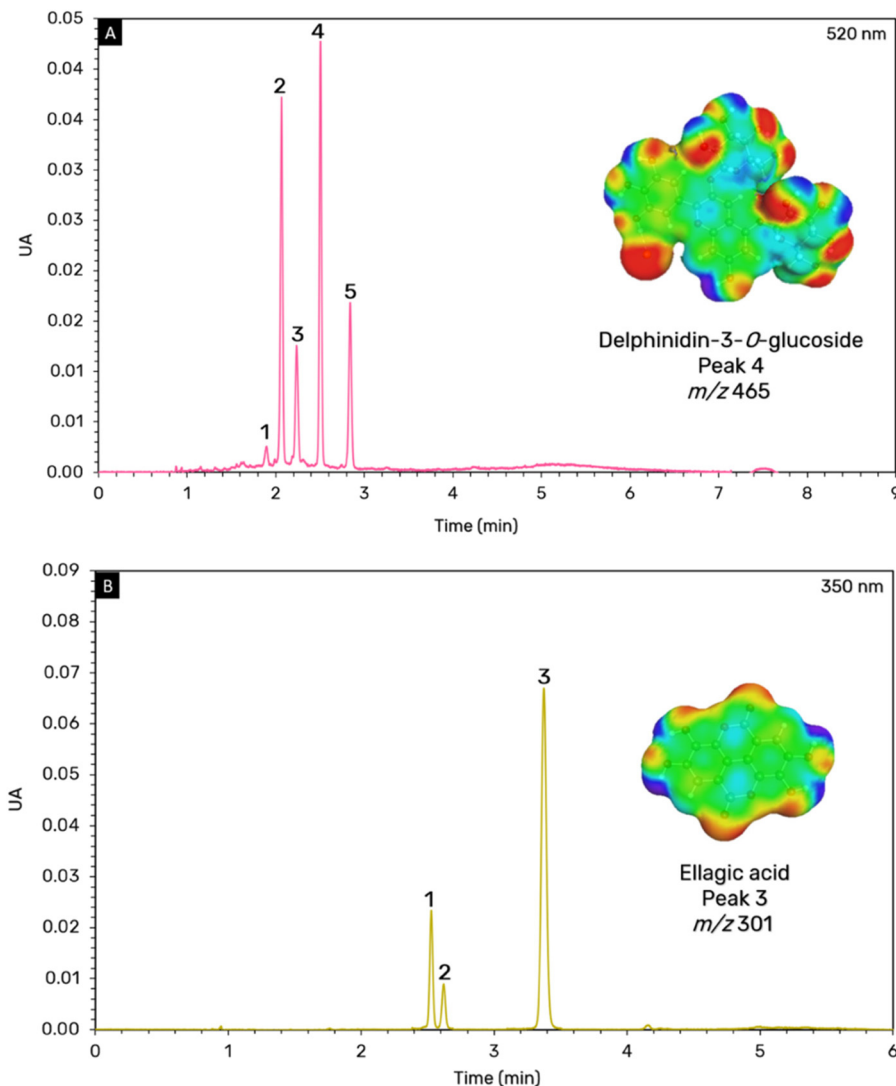
**COSMO-RS model.** COSMO-RS calculations were performed using a two-step procedure. First, using the software Turbomole (TmoleX19 version 4.5), the geometry of each molecule (HBA, HBD, anthocyanin, and ellagic acid as models) was optimized using COSMO-BP-TZVP (Fig. 1). Then, using the optimum designed molecules, the polarization charges ( $\sigma$ ) and

the surface composition functions,  $p(\sigma)$ , were calculated using COSMOtherm® software. For this, the COSMOtherm® (version 21.0) package with the parameterization BP\_TZVP\_21.ctd was used.<sup>30</sup> The COSMO-BP-TZVP model includes a base set of def-TZVP, DFT with the functional theory level B-P83, and the COSMO solvation model. Then, COSMO-RS was used to predict the activity coefficient at infinite dilution of anthocyanin models (delphinidin-3-*O*-glucoside and ellagic acid) in 10 512 combinations of HBAs and HBDs at 35 °C. Additionally, the  $\sigma$ -potentials and  $\sigma$ -profiles were obtained. The list of tested HBAs and HBDs is presented in Tables S1 and S2 from the ESI.†

**Experimental screening.** The criterion used to select the solvents experimentally tested was the activity coefficient at infinite dilution ( $\gamma^\infty$ ) exposed in COSMO-RS analysis. According to Hildebrand's solubility parameters theory,<sup>31</sup>  $\gamma^\infty$  is a precise parameter to describe the dissolution capability of a solute in a solvent. A small  $\gamma^\infty$  indicates that both substances are mutually soluble; therefore, the solvents with the lowest  $\gamma^\infty$  were selected to be experimentally tested. In addition, this selection was also made considering other issues like cost, availability, and toxicity. Thus, after the COSMO-RS screening, five bio-based solvents, six HBAs and HBDs were used to prepare the (D)ESs, and two ILs were selected. These are presented in Table 1. (D)ESs formed by two-component mixtures (HBA and HBD) were prepared based on the COSMO-RS screening results. Betaine and  $[\text{Ch}][\text{OAc}]$  were selected as HBAs, and 1,3-butanediol, urea, methyl urea, and 1,3-dimethyl urea were selected as HBDs. Ethanol, acetone, and methanol were used as control bio-based solvents; and cyrene and GVL were used as alternative bio-based solvents.

Regarding the preparation of the eutectic mixtures, for the screening assay, all (D)ESs were initially formulated using a molar ratio of HBA:HBD (molar ratio 1:2, considering each starting material's initial water content). Then, the mixtures were stirred in a hot metallic plate at 70 °C, with magnetic stirring of 250 rpm. The eutectic mixtures were prepared until a homogeneous and transparent liquid was obtained. The solvents were then stored for up to 24 h until use. Besides,  $[\text{Ch}][\text{OAc}]$  was used in an aqueous solution alone ( $C = 2 \text{ M}$ ), *i.e.*, without forming the eutectic mixture. The ILs and bio-based solvents were obtained commercially and diluted in water solutions ( $C = 2 \text{ M}$ ).

**Selecting the best solvents to extract anthocyanins, ellagic acid and its derivatives.** To select the best solvents to develop the biorefinery approach from pomegranate wastes, a screening assay was performed. Briefly, a Trayster (IKA digital) was used as the extraction method under the operational conditions fixed at 80 rpm, 25 min, at room temperature ( $\pm 23 \text{ °C}$ ) and SLR of  $0.16 \text{ mg}_{\text{biomass}} \text{mL}_{\text{solvent}}^{-1}$ . After the extraction, centrifugation was performed in a Thermo Fisher centrifuge (15 min, 4700g) to separate the extract from the residual biomass. Then, the supernatant, rich in the target compounds, was separated and characterized by UV-vis spectrophotometry and HPLC-PDA analysis. After selecting the best solvents to



**Fig. 1** HPLC chromatograms were recorded at 520 nm – anthocyanins, peak 1: delphinidin-3,5-O-diglucoside; peak 2: cyanidin-3-O-rutinoside; peak 3: pelargonidin-3-O-glucoside; peak 4: delphinidin-3-O-glucoside; and peak 5: cyanidin 3-O-glucoside (A), and at 350 nm – ellagic acid derivatives, peak 1:  $\alpha$ -punigalagin, peak 2:  $\beta$ -punigalagin, and peak 3: ellagic acid (B). The complete chemical information, including mass data, is depicted in Table S6 (ESI<sup>†</sup>). The 3D-induced surface charge density of delphinidin-3-O-glucoside and ellagic acid were obtained from COSMO-RS.

develop the biorefinery process, they were used for the optimization assays *via* the design of experiments (DoEs).

### Optimization of the extraction approach

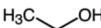
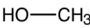
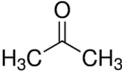
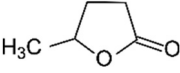

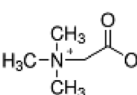
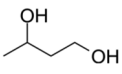
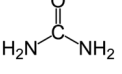
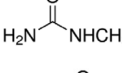
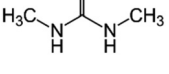
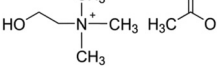
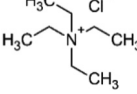
In this step, to maximize the extraction yield of anthocyanins and ellagic acid derivatives, four operational conditions were tested in a central composite rotatable design approach (CCRD  $2^4$  + axial points + central points). The operational variables chosen for optimization were: ( $X_1$ ) SLR, in  $\text{mg}_{\text{biomass}} \text{mL}_{\text{solvent}}^{-1}$ ; ( $X_2$ ) concentration of the solvent –  $C$ , in mM; ( $X_3$ ) pH; and ( $X_4$ ) time of extraction –  $t_{\text{ext}}$ , in min. The responsive variables optimized were the yields of anthocyanins and ellagic acid ( $\text{mg}_{\text{anthocyanins}} \text{g}_{\text{biomass}}^{-1}$  and  $\text{mg}_{\text{ellagic acid}} \text{g}_{\text{biomass}}^{-1}$ , respectively). Statistica 14.0.15 software performed the DoEs and generated responsive surface plots. Tables S3

and S4 (ESI<sup>†</sup>) describe the encoded and experimental variables of the optimization assay of the anthocyanins, ellagic acid, and its derivatives, respectively. Two sequential routes of extraction were suggested: first, recovering anthocyanins and then ellagic acid and its derivatives; second, extracting first ellagic acid and its derivatives and then anthocyanins. The criterion for selecting the best route was selectivity, *i.e.*, those with a higher purity of a specific pigment.

### Quantification and identification of anthocyanins, ellagic acid and its derivatives

**UV-vis spectrophotometry.** The quantification of anthocyanins was performed following the methodology of pH differential.<sup>32</sup> Briefly, potassium chloride buffer (pH 1.0) and 0.4 M sodium acetate buffer (pH 4.5) were prepared and separately

**Table 1** Chemical structure, molecular formula, and molecular weight of the starting materials used to produce the eutectic mixtures (HBAs and HBDs), biobased solvents, and ionic liquids (ILs)

Chemical name	Chemical structure	Molecular formula	Molar mass (g mol <sup>-1</sup> )
Ethanol (EtOH) – bio-based solvent		C <sub>2</sub> H <sub>6</sub> O	46.06
Methanol (MeOH) – bio-based solvent		CH <sub>4</sub> O	32.04
Acetone – bio-based solvent		C <sub>3</sub> H <sub>6</sub> O	58.08
Gamma-valerolactone (GVL) – bio-based solvent		C <sub>5</sub> H <sub>8</sub> O <sub>2</sub>	100.12
Cyrene – bio-based solvent		C <sub>6</sub> H <sub>8</sub> O <sub>3</sub>	128.13
Betaine – HBA		C <sub>5</sub> H <sub>11</sub> NO <sub>2</sub>	117.15
1,3-Butanediol – HBD		C <sub>4</sub> H <sub>10</sub> O <sub>2</sub>	90.12
Urea – HBD		CH <sub>4</sub> N <sub>2</sub> O	60.06
Methyl urea – HBD		C <sub>2</sub> H <sub>6</sub> N <sub>2</sub> O	74.08
1,3-Dimethyl urea – HBD		C <sub>3</sub> H <sub>8</sub> N <sub>2</sub> O	88.11
Cholinium acetate ([Ch][OAc]) – IL and HBA		C <sub>7</sub> H <sub>17</sub> NO <sub>3</sub>	163.21
Tetraethylammonium chloride ([N <sub>2,2,2,2</sub> ][Cl]) – IL		C <sub>8</sub> H <sub>20</sub> NCl	165.70

added to the anthocyanin-rich extract. Then, the concentration of anthocyanins was calculated following eqn (1) and (2).

$$A = (A_{520} - A_{700})_{\text{pH } 1.0} - (A_{520} - A_{700})_{\text{pH } 4.5} \quad (1)$$

$$\text{Anthocyanins (mg g}^{-1}\text{)} = \frac{(A \times \text{MW} \times \text{DF} \times 1000)}{l \times \epsilon \times g_{\text{biomass}}} \quad (2)$$

$A_{520}$  and  $A_{700}$  represent the absorbance at 520 nm and 700 nm, respectively; MW is the molecular weight of the main anthocyanin extracted from pomegranate wastes (delphinidin-3-O-glucoside = 500.83 g mol<sup>-1</sup>); DF is the dilution factor (15×),  $\epsilon$  is the extinction molar coefficient for delphinidin-3-O-glucoside (27 300), and  $l$  is the path length (cm). The total anthocyanin content was expressed by mg<sub>anthocyanins</sub> g<sub>biomass</sub><sup>-1</sup>.

The quantification of the ellagic acid and its derivatives was performed using a calibration curve of an external standard of

ellagic acid diluted in [Ch][OAc] aqueous solution (350 nm,  $r^2 > 0.99$ , 0.005–0.0625 mg<sub>ellagic acid</sub> mL<sup>-1</sup>). Each assay's total concentration of ellagic acid and its derivatives was expressed in mg<sub>ellagic acid</sub> g<sub>biomass</sub><sup>-1</sup>.

**Identification of compounds by HPLC-PDA-MS.** All the obtained extracts were analyzed by high-performance liquid chromatography combined with a photodiode array detector and tandem mass spectrometry (HPLC-PDA-MS). The chromatographic analysis was performed on a Kinetex C<sub>18</sub> column (150 × 4.6 mm, 2.6 μm, Phenomenex, Torrance, CA, USA). The anthocyanins were characterized at 520 nm using a chromatographic method composed of a binary mobile phase: (A) water + 0.25 mol L<sup>-1</sup> citric acid and (B) ethanol – HPLC grade – at a flow rate of 1 mL min<sup>-1</sup> with the column temperature fixed at 55 °C and a gradient flow as follows: 0 min (90% A), 1.5 min (85% A), 2 min (85% A), 2.2 min (84% A), 2.3 min (83% A), 2.5 min (80% A), 2.75 min (78% A), 3.0 min (78% A), 3.5 min



(75% A), 4.0 min (75% A), 4.25 min (74% A), 4.5 min (73% A), 4.75 min (75% A), 5.0 min (65% A), 6.0 min (90% A), and 9.0 min (90% A – reconditioning time).<sup>33</sup> In addition, using the same chromatographic column, the ellagic acid-rich extract was characterized at 350 nm, with the column temperature fixed at 42 °C, a flow rate of 1.0 mL min<sup>−1</sup>, and a binary mobile phase composed of (A) water and (B) acetonitrile, both added with 0.1% v/v of acetic acid. The gradient flow was: 0 min (98% A), 0.30 min (90% A), 1.5 (85% A), 1.90 min (75% A), 2.0 min (72% A), 2.1 min (70% A), 2.35 min (70% A), 2.4 min (69% A), 2.5 min (67% A), 2.8 min (65% A), 2.9 (60% A), 3.5 min (60% A), and 6 min (98% A – reconditioning time).

MS and MS<sup>2</sup> scans were conducted in positive ionization mode for anthocyanins and negative ionization mode for ellagic acid derivatives (100–1500 Da). The operational conditions were as follows: flow rate of 0.5 mL min<sup>−1</sup>, capillary voltage between 25 and 35 V, spray voltage of 5–7 kV, tube lens offset of 75 V, capillary temperature of 250–300 °C, and sheath gas (N<sub>2</sub>) flow rate set to 8 arbitrary units. Data acquisition and processing were performed using Xcalibur software (version 2.2 SPI.48).<sup>34</sup>

### Biochar production and characterization

An alternative method based on eutectic solvent was proposed to produce a biochar material.<sup>35</sup> Briefly, a (D)ES was prepared by mixing cholinium chloride as HBA and oxalic acid as HBD ([Ch]Cl:OA, molar ratio 1:2, without adding water) under magnetic stirring (200 rpm) at 70 °C. The choice of applying [Ch]Cl:OA at 1:2 molar ratio (HBA:HBD) was based on a previous article from our research group.<sup>36</sup> Then, in a pressure resistance flask, the residual biomass used after pigment extraction (anthocyanins and ellagic acid) was placed in contact with [Ch]Cl:OA under constant stirring (200 rpm), and at an SLR of 0.1 g<sub>biomass</sub> mL<sub>(D)ES</sub><sup>−1</sup>, and with the temperature fixed at 120 °C. After 60 minutes, the system was cooled down in an ice bath, and the obtained material was washed with distilled water and centrifuged (15 min, 4700g). The supernatant phase was rich in the (D)ES and could be recovered after the water had evaporated. Then, the biochar material was obtained in the precipitated fraction after centrifugation, and was placed into an oven at 55 °C until completely dry, and a black powder was obtained.

The biochar morphology was assessed by scanning electron microscopy (SEM, SU-70, Hitachi). Dry samples were placed onto a metal stub, coated with a thin gold layer using a sputter coater (SEM Coating Unit E5000, Polaron), and analyzed with an accelerating voltage of 15 kV. The surface area was determined using a Brunauer-Emmett-Teller (BET) method using a Gemini VII from the Micrometrics instrument, based on the adsorption-desorption isotherms of N<sub>2</sub> at 77 K. The elemental analysis of biochar samples was conducted with a TruSpec series 200–200 elemental analyzer (Michigan, USA). The combustion furnace and after-burner temperatures were maintained at 1075 °C and 850 °C, respectively. The difference determined the oxygen content. These results were used to calculate the atomic H/C, O/C, and (O + N)/C ratios to assess the

relationships concerning the relative degree of hydrophobicity of the produced biochar material. Biochar's infrared spectra (FTIR) spectra were obtained with a resolution of 4 cm<sup>−1</sup> over a wavenumber range of 4000 to 400 cm<sup>−1</sup> with 64 scans. Spectral analysis was performed using SpectralSoft Software (PerkinElmer Spectrum BX spectrometer). The integrity of [Ch]Cl:OA used for biochar production was assessed using Thermogravimetric Analysis (TGA). Thermal decomposition temperatures were measured with a Mettler Toledo TGA/DSC system (Schwerzenbach, Switzerland). The samples were heated at a rate of 10 °C min<sup>−1</sup>, across a temperature range of 30 to 500 °C. Approximately 5 mg of [Ch]Cl:OA was carefully placed into an aluminium crucible and analyzed under a nitrogen atmosphere with a flow rate of 50 mL min<sup>−1</sup>.

### Biochar utilization and the removal of synthetic dyes from aqueous solution

As a proof of concept to show potential application of the biochar material produced in this work, the removal of dyes from water was investigated. Food (sunset yellow, tartrazine yellow, brilliant blue, and red 40) and textile (indigo carmine blue, chloranilic acid, and rhodamine) dyes were used in adsorption experiments (see Table S5 for more chemical details – ESI†). For that purpose, a concentrated aqueous solution of each dye was prepared (0.025 mg<sub>dye</sub> mL<sub>solution</sub><sup>−1</sup>), and their initial absorbance (UV-vis) was evaluated and considered as the initial concentration (A<sub>0</sub>). Then, the adsorption experiments were conducted under constant stirring (60 rpm) for 75 min. After that, a centrifugation step (5 min, 4700g) was performed to precipitate the biochar. The supernatant solution was analyzed again by UV-vis (A<sub>1</sub>) to calculate the amount of dye adsorbed by the biochar material, as detailed in eqn (3). All experiments were conducted in triplicate and expressed as the mean of %<sub>dye adsorption</sub> ± standard deviation.

$$\%(\text{dye adsorption}) = 100 - \frac{(A_1 \times 100)}{A_0} \quad (3)$$

### Greenness assessment of the biorefinery by using the Path2Green metric

The greenness assessment of the developed biorefinery was evaluated by using the Path2Green metric.<sup>37</sup> This metric is based on 12 principles of green extraction. In this metric, parameters are established by evaluating attributes throughout the pre- and post-extraction procedures: 1: Biomass; 2: Transport; 3: Pre-treatment; 4: Solvents; 5: Scaling; 6: Purification; 7: Yield; 8: Post-Treatment; 9: Energy; 10: Application; 11: Repurposing, and 12: Waste Management. Each principle is scored between −1.00 and +1.00, with a score closer to +1.00, indicating better adherence to the green principle. Also, each principle was evaluated individually, with the environmental aspect carrying a more pronounced weight (weight 3), followed by society (weight 2), and economy (weight 1). The Path2Green cellphone app made the evaluation and depicted the final pictogram of the metric. The result pictogram indicates the final

score and the performance of the extraction process, allowing the perception of red flags, by which the developed process can be improved in terms of sustainability.

## Results and discussion

### Chemical characterization of pomegranate waste

To identify the target compounds in the pomegranate waste, extracts using MeOH 80% at pH 3 and 10 were prepared and analyzed by HPLC-PDA-MS/MS. By processing the chromatogram at 520 nm, five well-defined peaks were obtained in the acid extract (Fig. 1A). Their proposal identification was recorded in Table S6 (ESI†) based on previous studies.<sup>33,38</sup>

Three aglycones were extracted: cyanidin, pelargonidin, and delphinidin. The major peak (peak 4 Fig. 1A) was identified as delphinidin-3-O-glucoside ( $m/z$  465,  $ms^2$  303 –  $[M - H - 162]^-$ ). In the alkaline extract, ellagic acid derivatives were identified, mainly represented by ellagic acid aglycone ( $m/z$  301) – peak 3 (Fig. 1B) and the derivatives,  $\alpha$ -punicalagin and  $\beta$ -punicalagin, (both with  $m/z$  1083) – peaks 1 and 2 from Fig. 1B, respectively. After obtaining detailed knowledge of the target composition of the biomass, the extraction process variables were optimized to yield these compounds selectively and efficiently. The macro-compositional analysis of pomegranate waste, as presented in Table S7 (ESI†), highlights its high fiber and carbohydrate content. These characteristics make pomegranate waste particularly suitable for biochar production. The significant fiber content, averaging  $22.00 \pm 7.02\%$ , provides a strong structural framework, while the carbohydrate content, averaging  $26.70 \pm 6.42\%$ , supports the formation of carbon-rich biochar. These properties are key for developing efficient adsorbent materials, as discussed in the following sections.

### COSMO-RS screening of solvents

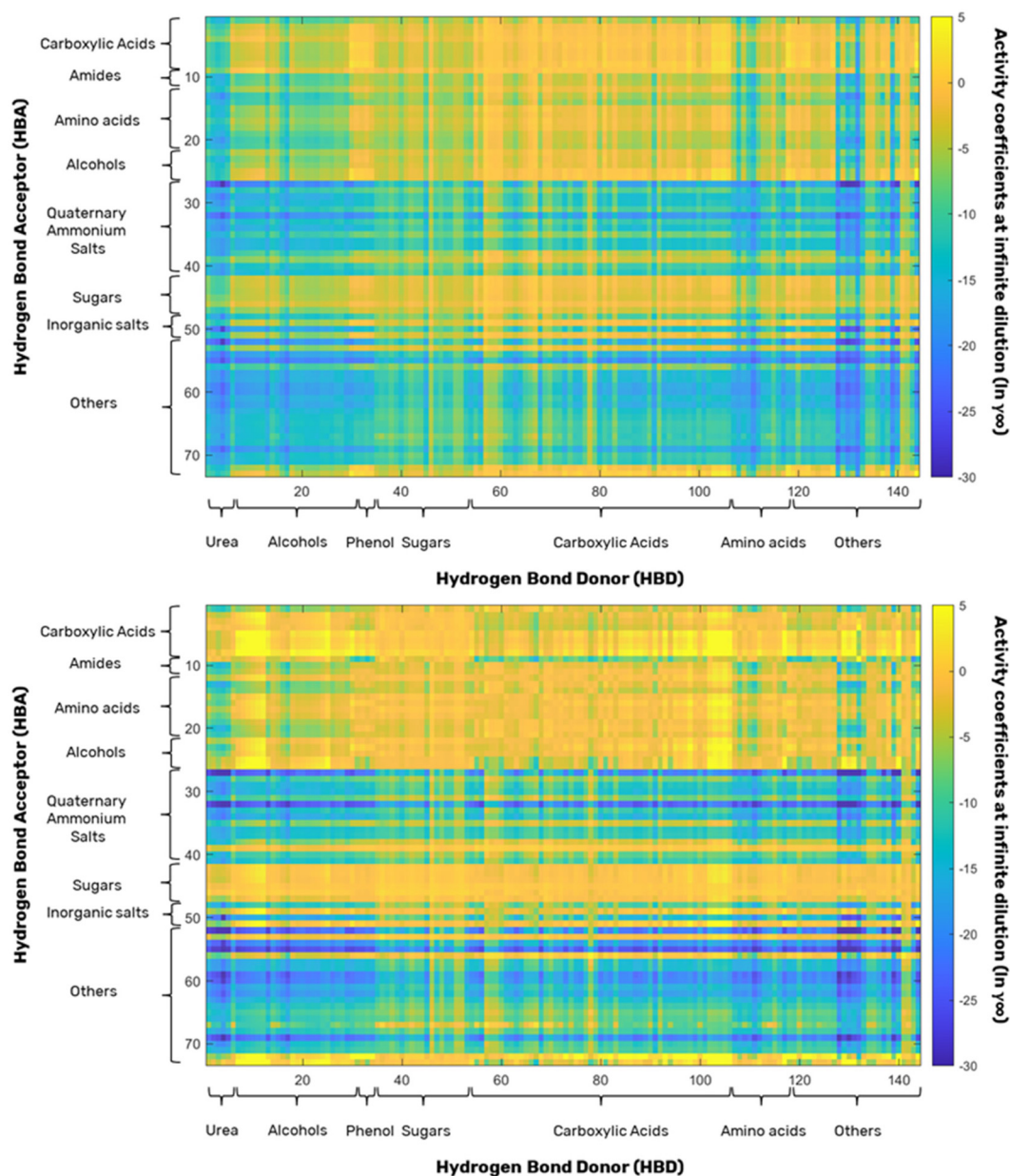
Due to the extensive range of HBA and HBD combinations that can form a (D)ES, COSMO-RS was employed as a screening tool to predict the best HBA and HBD pairs for extracting the primary pigments (anthocyanins and ellagic acid-rich fraction) from pomegranate waste. Following the characterization of the biomass, two target molecules, (i) delphinidin-3-O-glucoside and (ii) ellagic acid (Fig. 1A and B), were chosen as model compounds due to their high concentration in the biomass. The infinite dilution activity coefficient ( $\gamma^\infty$ ) was used to evaluate the solubility behavior of the solute in various HBA and HBD combinations.<sup>39</sup> This coefficient is a molecular descriptor to pre-select the best HBA and HBD pairs. The  $\gamma^\infty$  values were estimated for combinations of 73 HBAs and 144 HBDs in a molar ratio of 1 : 2 at 35 °C, resulting in 10 512 possible combinations. Besides these mixtures, 49 pure biobased solvents were also investigated. The results are depicted in Fig. 2, where the  $\ln \gamma^\infty$  values are shown using a color scale. Since a lower  $\ln \gamma^\infty$  value indicates higher solubility, the relationship is inversely proportional.<sup>39</sup>

As shown in Fig. 2, quaternary ammonium salts exhibit low  $\ln \gamma^\infty$  values, suggesting high solubility for ellagic acid and delphinidin-3-O-glucoside, especially for  $[Ch][OAc]$  and  $[N_{2,2,2,2}]Cl$ , regardless of the HBD. Additionally, Fig. 2 reveals negative  $\ln \gamma^\infty$  values for certain HBA groups, notably betaine. Regarding the HBDs, compounds like urea and the alcohol group show low  $\ln \gamma^\infty$  values. Conversely, HBAs such as carboxylic acids and sugars have high  $\ln \gamma^\infty$  values, indicating poor solubility for the target compounds, regardless of the HBD. Moreover, this study suggests that HBA has a more significant impact on the solubilization of the target compounds than HBD. This conclusion is supported by the lines in Fig. 2, which show that the  $\ln \gamma^\infty$  value remains approximately constant for each HBA, irrespective of the HBD.

For the bio-based solvents (Table S8 – ESI†), those that exhibited the lowest  $\ln \gamma^\infty$  values for delphinidin-3-O-glucoside and ellagic acid were cyrene and GVL. Therefore,  $[Ch][OAc]$  and  $[N_{2,2,2,2}]Cl$  combined with urea and 1,3-butanediol were selected for subsequent experimental screening. In Fig. S1 (ESI†), it is possible to see the  $\sigma$ -profiles and  $\sigma$ -potential ( $\mu(\sigma)$ ) of the selected solvents (considered optimal for being tested in the experimental screening). Additionally, the bio-based solvents GVL and cyrene were also selected.

### Solid-liquid extraction—experimental screening assay

Based on the results of the previous section, the best alternative eco-friendly solvents were experimentally screened regarding their capacity to extract anthocyanins, ellagic acid, and its derivatives from pomegranate waste. Considering the results depicted in Fig. 3, the aqueous solution of GVL (2 M) was the most efficient solvent tested, allowing the recovery of  $19.78 \pm 0.75 \text{ mg}_{\text{anthocyanins}} \text{ g}_{\text{biomass}}^{-1}$ , which represents a performance of almost 6-fold higher comparing with water, and 2-fold higher when compared with methanol (MeOH 100%). Although a new bio-based solvent, GVL is already produced on a large scale in Europe,<sup>40</sup> offering an excellent opportunity to replace petroleum-based solvents. Today, GVL is used to solubilize polymers, cosmetics, agrochemicals, and pharmaceuticals and as a cleaning agent in various paint and coating formulations.<sup>40</sup> In addition, due to their characteristic aroma, GVL could be used as a perfume ingredient or as an additive in foods and beverages.<sup>41</sup> Most importantly, GVL has low (or negligible) toxicological potential, allowing its use in the most varied sectors. Considering the feasibility of an extraction process, GVL is a promising alternative to organic solvents for showing low-vapor pressure, which minimizes its loss by evaporation (associated with air contamination and lower solvent performance). Compared to (D)ES-mediated processes, GVL has the advantage of being easier to handle, which means that the solvent formulation is not required. Fig. 3 also shows that other tested alternative solvents, namely, those formulated using  $[Ch][OAc]$  and  $[N_{2,2,2,2}]Cl$  as HBA, and their combination with urea derivatives as HBD, presented a satisfactory extraction performance. However, they present a poorer performance in terms of being selective for anthocyanins, being thus responsible for the co-extraction of large amounts of ellagic



**Fig. 2** The activity coefficients at infinite dilution ( $\ln \gamma^\infty$ ) of delphinidin-3-O-glucoside (top) and ellagic acid (bottom) in eutectic mixtures (1 : 2) at 35 °C. Tables S1 and S2 from the ESI† contain the label of each compound analyzed.

acid and its derivatives (between 5 and 10  $\text{mg}_{\text{ellagic acid}} \text{g}_{\text{biomass}}^{-1}$ ). To develop a green multiproduct biorefinery, a high selectivity is desired to minimize post-purification steps when a mix of target compounds is recovered in one fraction.<sup>42</sup> For these reasons, the aqueous solution of GVL was selected as a solvent for the design of experiments applied in this work with the objective of finding the optimal conditions that maximize the recovery of anthocyanins.

In a second step, after recovering anthocyanins, the same biomass was used to recover a rich fraction of ellagic acid and its derivatives – pigments with a bright yellow color. As depicted in Fig. 3, [Ch][OAc]-based solutions performed better than VOSs and bio-based solvents. Here, [Ch][OAc] was used as

HBA in (D)ES formulations and as a single component in aqueous solution. [Ch][OAc] is considered a bio-IL, already used as a promising solvent in the extraction of value-added compounds<sup>43</sup> and as a separation agent in the chemical industry, including gas absorption and liquid–liquid extraction.<sup>44</sup> Fig. 3 shows that the best yield of extraction was obtained using the (D)ES composed of [Ch][OAc]:urea (molar ratio – 1 : 2),  $10.31 \pm 1.21 \text{ mg}_{\text{ellagic acid}} \text{g}_{\text{biomass}}^{-1}$ . However, the aqueous solution of [Ch][OAc] (2 M) achieved an equivalent extraction yield,  $9.74 \pm 1.23 \text{ mg}_{\text{ellagic acid}} \text{g}_{\text{biomass}}^{-1}$ . Thus, considering the advantages of using an aqueous solution rather than a eutectic mixture, the optimization process was performed using an aqueous solution of [Ch][OAc]. Besides, this



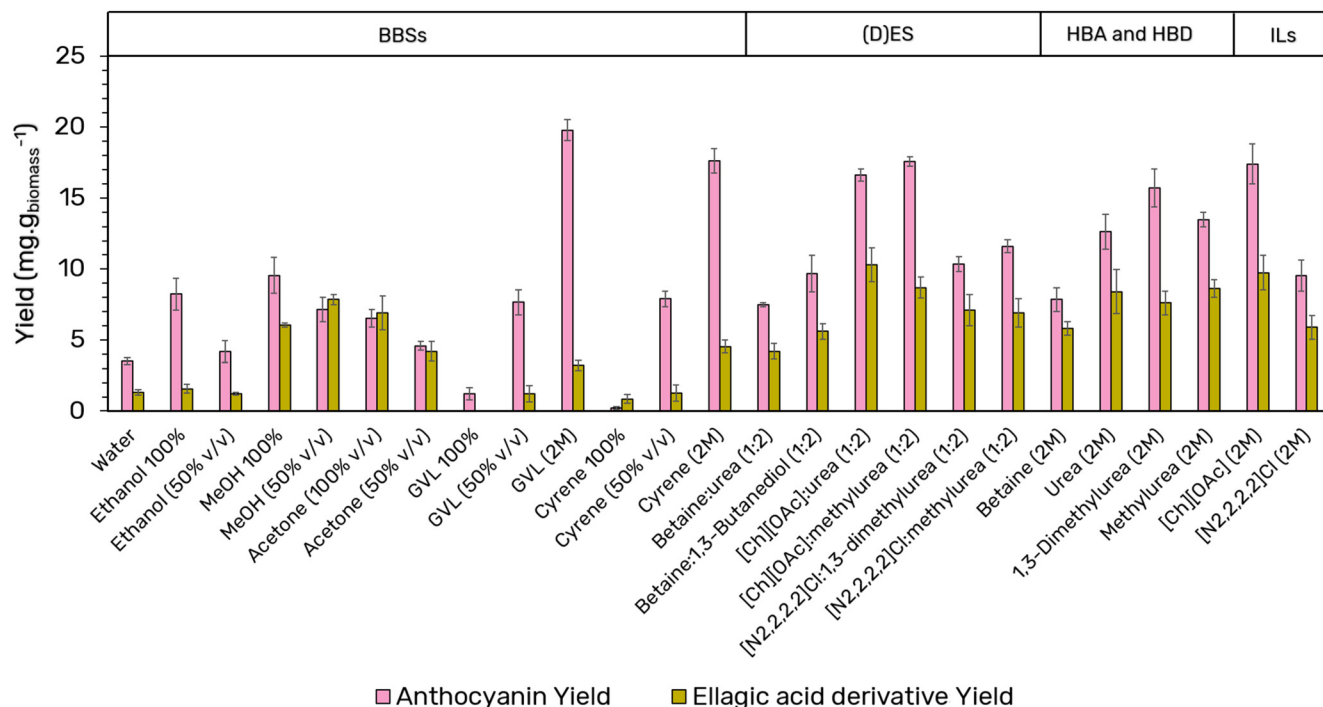


Fig. 3 Screening of different solvent families upon their ability to extract anthocyanins, ellagic acid and its derivatives from pomegranate waste. (MeOH – methanol; GVL – gamma-valerolactone; [Ch][OAc] – cholinium acetate; [N<sub>2,2,2,2</sub>]Cl – tetraethylammonium chloride.)

choice is allied with several health benefits associated with [Ch][OAc], mainly regarding its effect on gut microbiota, neurotransmitter synthesis, cell-membrane signalling, lipid transport, and methyl-group metabolism.<sup>45</sup>

#### Solid-liquid extraction—process optimization

After selecting the most promising solvents to recover the target compounds from pomegranate waste, two sequential design experiments (DoE) were performed; the first for recovering anthocyanins using GVL, and the second using an aqueous solution of [Ch][OAc] to obtain a rich fraction of ellagic acid and its derivatives. As mentioned in the previous section, since GVL promoted selective extraction of anthocyanins (which means extracting high amounts of anthocyanin and low amounts of ellagic acid and its derivatives), we started the extraction by recovering the anthocyanins and then the ellagic acid derivatives. In both DoE analyses, a central composite rotatable design (CCRD) was applied. Four independent variables (operational variables) were evaluated ( $2^4$  + axial and central points): solid-liquid ratio ( $X_1$ : SLR,  $\text{g}_{\text{biomass}} \text{mL}_{\text{solvent}}^{-1}$ ), the concentration of the solvent ( $X_2$ : C, M), pH ( $X_3$ ), and the time of extraction ( $X_4$ :  $t_{\text{ext}}$ , min). The responsive variables that guided the optimization process were the yield of anthocyanins, ellagic acid, and its derivatives. The assays' real (experimental) and encoded values can be viewed in Tables S3 and S4 (ESI†).

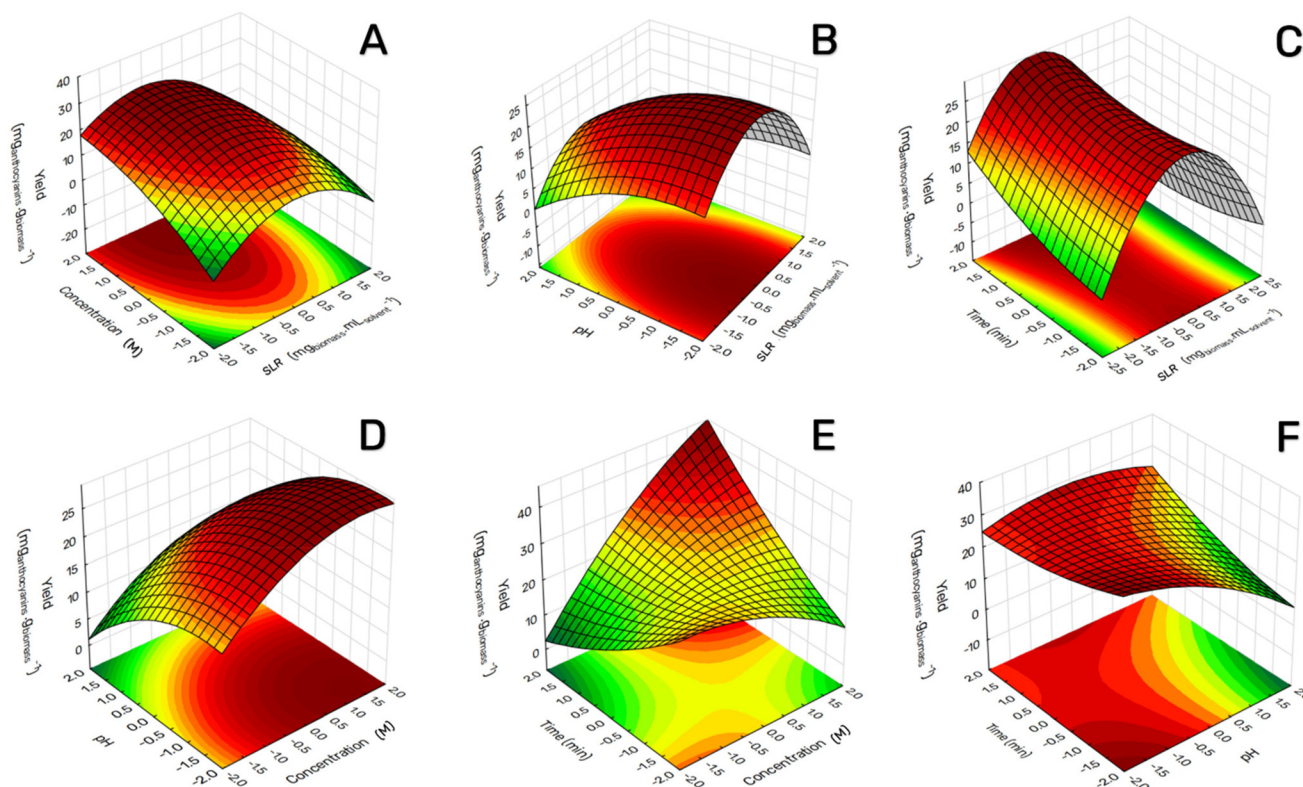
#### Optimization of anthocyanin recovery

A response surface methodology (RSM) was used to optimize the operational conditions and maximize anthocyanin extrac-

tion yields ( $\text{mg}_{\text{anthocyanins}} \text{g}_{\text{biomass}}^{-1}$ ). The RSM allowed the exploration of the relationship between the four studied variables. Pareto's chart showed the most relevant interaction between the conditions studied (Fig. S2, ESI†). The ESI presents all the experimental results obtained and the optimized variables (Table S3 – ESI†), with the extraction yield ranging between 1.53 and 35.69  $\text{mg}_{\text{anthocyanins}} \text{g}_{\text{biomass}}^{-1}$  and the predicted vs. observed values are shown in Fig. S3† (statistical significance of the variables and their interactions highlighted satisfying predictability at a confidence level of 95% ( $R^2 = 0.76$ )). Eqn (4) shows the impact of these four variables on recovering anthocyanins from pomegranate waste, which was fitted concerning the results of the analysis of variance (ANOVA).

Fig. 4 depicts the main results obtained from the predictive model, with all variables fully optimized since concave surfaces delimited hot spot zones (dark red zones), where a maximum yield is predicted. It shows that the best operational conditions to recover a high yield of anthocyanins from pomegranate waste are SLR = 0.07  $\text{g}_{\text{biomass}} \text{mL}_{\text{solvent}}^{-1}$ ; concentration of GVL of 2.9 M; acidic pH (around pH 2); and time of extraction of 30 min (at 80 rpm). By comparing the experimental and predicted data achieved for the extraction yield under the selected conditions, a relative deviation of 3.05% was observed (Table S9 from the ESI†), and an optimum yield of  $38.52 \pm 0.06 \text{ mg}_{\text{anthocyanins}} \text{g}_{\text{biomass}}^{-1}$ , proving that the fitted model has high accuracy and precision.

Using GVL as an extraction solvent offers numerous advantages, particularly in the context of ready-to-use extracts.<sup>46</sup>



**Fig. 4** Factorial planning ( $2^4$ ): response surface plots regarding the yield of extraction of anthocyanins from pomegranate waste ( $\text{mg}_{\text{anthocyanins}} \text{g}_{\text{biomass}}^{-1}$ ) with the combined effects of (A) SLR and C, (B) SLR and pH, (C) SLR and  $t_{\text{ext}}$ , (D) C and pH, (E) C and  $t_{\text{ext}}$ , and (F) pH and  $t_{\text{ext}}$  using different aqueous solutions of gamma-valerolactone (GVL) as extractant media. SLR = solid–liquid ratio, C = concentration and  $t_{\text{ext}}$  = time of extraction.

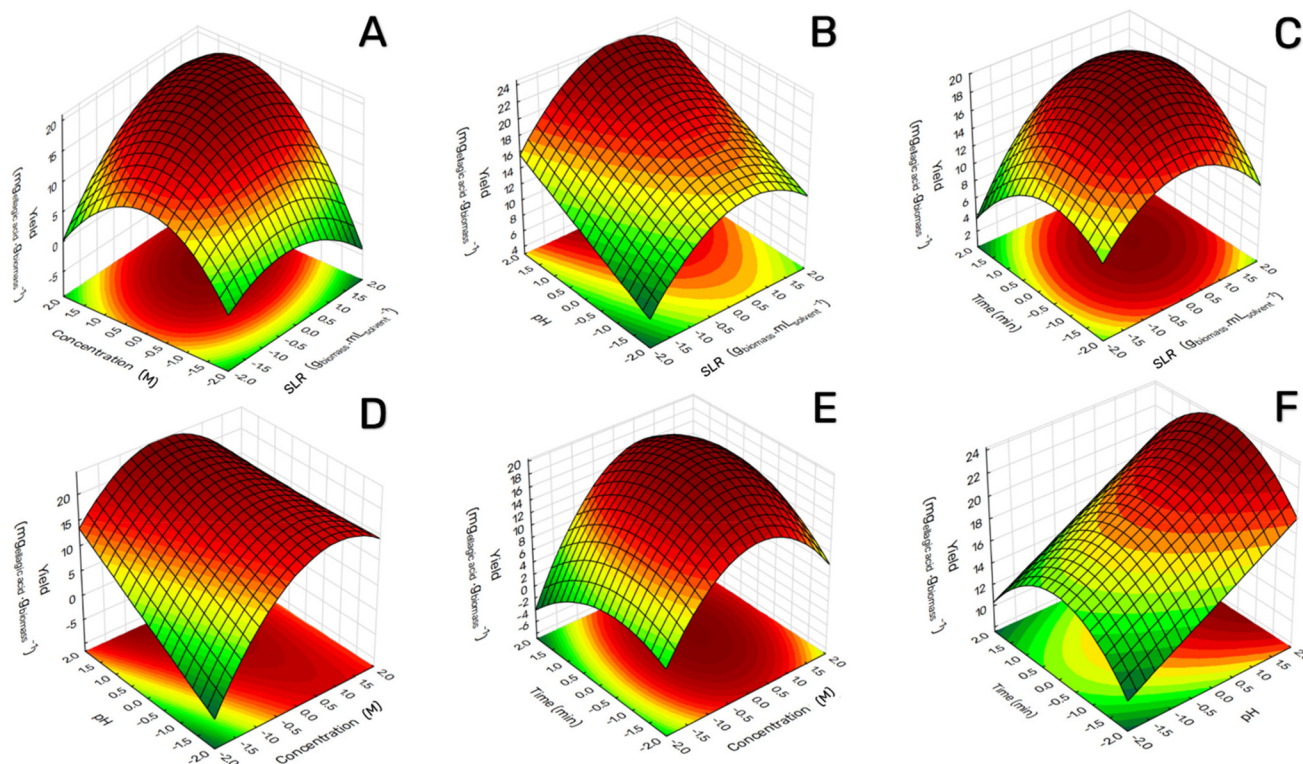
GVL, a bio-based solvent, has already been successfully applied to recover natural bioactive compounds from biomass, including pigments like carotenoids, phenolic acids, and flavonoids.<sup>47,48</sup> Recently, an aqueous GVL solution (150 mM) was used to extract carotenoids from haloarchaeal bacteria.<sup>47</sup> Unlike anthocyanins, which are water-soluble pigments, carotenoids are hydrophobic compounds, further showcasing the versatility of GVL when used in aqueous solutions (depending on the concentration used – which must be optimized to each target compound). This adaptability makes GVL an excellent alternative to petrochemical solvents, contributing to greener extraction processes, which indeed have been explored and pointed out as a sustainable strategy for biomass pre-treatment.<sup>49</sup> Additionally, GVL has proven to be an effective preservative, maintaining the stability and shelf life of the extracted carotenoids even at elevated temperatures (96 °C).<sup>47</sup> Another significant benefit is GVL's regulatory approval by international agencies (International Fragrance Association – IFRA, Flavor and Extract Manufacturers Association Generally Recognized As Safe – FEMA GRAS/FDA guidelines), allowing its use as an active ingredient in fragrance and perfume formulations. These properties make GVL a highly promising solvent for sustainable applications across various industries, from cosmetics to cleaning and flavoring agents. In this scenario, using a solvent that does not need to be removed from the

extract can also significantly reduce costs associated with further purification and polishing techniques, which are typically required when the solvent imposes restrictions on the final applications.<sup>21</sup> By eliminating the need for solvent removal, the overall process becomes more efficient and cost-effective, making it an attractive option for industries aiming to streamline production while ensuring product safety and quality.

$$\begin{aligned}
 Y(\text{anthocyanin yield}) = & 24.13 - 2.07(X_1) - 4.11(X_1)^2 \\
 & + 3.08(X_2) - 1.15(X_2)^2 - 3.73(X_3) - 1.17(X_3)^2 \\
 & + 1.02(X_4) + 0.63(X_4)^2 - 1.06(X_1 \times X_2) \\
 & - 0.92(X_1 \times X_4) + 3.85(X_2 \times X_4) + 1.69(X_3 \times X_4)
 \end{aligned} \quad (4)$$

#### Optimization of the extraction of ellagic acid and its derivatives

Using the same biomass after anthocyanins' extraction, a second DoE was performed to maximize the yield of extraction of ellagic acid derivatives ( $\text{mg}_{\text{ellagic acid}} \text{g}_{\text{biomass}}^{-1}$ ), using an aqueous solution of [Ch][OAc] as the extraction solvent. The same operational variables were evaluated and described in Table S4 (ESI†). All tested variables were considered significant to a predictive model, with the concentration of [Ch][OAc] being the most representative, followed by the pH and SLR



**Fig. 5** Factorial planning ( $2^4$ ): response surface plots regarding the yield of extraction of ellagic acid and derivatives from pomegranate waste ( $\text{mg}_{\text{ellagic acid}} \text{g}_{\text{biomass}}^{-1}$ ) with the combined effects of (A) SLR and C, (B) SLR and pH, (C) SLR and  $t_{\text{ext}}$ , (D) C and pH, (E) C and  $t_{\text{ext}}$ , and (F) pH and  $t_{\text{ext}}$  using different aqueous solutions of  $[\text{Ch}][\text{OAc}]$  as the solvent. SLR = solid–liquid ratio, C = concentration and,  $t_{\text{ext}}$  = time of extraction.

(Pareto's chart – Fig. S4, ESI†), with the extraction of ellagic acid and derivatives ranging from  $23.78 \text{ mg}_{\text{ellagic acid}} \text{g}_{\text{biomass}}^{-1}$  to  $4.41 \text{ mg}_{\text{ellagic acid}} \text{g}_{\text{biomass}}^{-1}$ . The model provided by eqn (5) expressed the predicted values, which has a 95% confidence level, with  $F_{\text{calculated}} > F_{\text{tabulated}}$  (16-fold higher) and  $R^2 = 0.77$ , highlighting a high-predictable model, as shown in Fig. S5 from the ESI†. The surface responsive plots are shown in Fig. 5, showing a complete optimization of the variables SLR and C, with optimum values of  $0.07 \text{ g}_{\text{biomass}} \text{ mL}_{\text{solvent}}^{-1}$ , and  $2.9 \text{ M } [\text{Ch}][\text{OAc}]$ . The time was also fully optimized, reaching a maximum extraction yield at 55 min. Unlike for the anthocyanins, the optimum pH for the efficient extraction of ellagic acid and derivatives was alkaline (pH 13). A model validation experiment was performed using the optimized operational conditions (Table S10 in the ESI†). The optimum extraction yield obtained in the validation assay was  $21.82 \text{ mg}_{\text{ellagic acid}} \text{g}_{\text{biomass}}^{-1}$ , corresponding to a relative deviation of 1.72% from the predicted value. This outstanding result suggests the high confidence and accuracy of the predictive model designed by the CCRD ( $2^4$ ).

Regarding the use of cholinium-based ILs, it is true that, in recent years, they have been regarded as sustainable solvents. However, this is not entirely accurate.<sup>50</sup> While cholinium-based ILs are certainly a better alternative to volatile organic solvents, which have significant production issues and safety concerns for handlers, their sustainability can still be ques-

tioned. A key point of discussion is that  $[\text{Ch}][\text{OAc}]$  already has a biological production pathway, yet the market continues to commercialize synthetic versions, which come with their own production-related challenges. In this context, it is important to address the trend of persisting with synthetic cholinium-based ILs. While cost-effectiveness may be a driving factor for manufacturers, promoting the use of synthetic routes is not something we can encourage, especially given the availability of greener alternatives. Furthermore,  $[\text{Ch}][\text{OAc}]$  has proven to be an effective solvent for extracting ellagic acid derivatives from pomegranate and has been widely used as a co-solvent to enhance drug solubility, stability, and bioavailability.<sup>51,52</sup> Its applications extend to drug formulation, delivery systems, and even the extraction of active pharmaceutical ingredients (APIs) from natural sources. Thus, the optimized approach developed in this study offers a win-win solution compared to conventional methods. It not only provides a more sustainable extraction process but also harnesses the potential of  $[\text{Ch}][\text{OAc}]$  to enhance the quality of bioactive compounds, as demonstrated in pharmaceutical applications.<sup>53</sup>

$$\begin{aligned}
 Y(\text{ellagic acid yield}) = & 19.72 + 1.41(X_1) - 1.45(X_1)^2 \\
 & + 2.47(X_2) - 2.73(X_2)^2 + 2.25(X_3) - 1.22(X_4)^2 \\
 & + 1.23(X_1 \times X_2) + 0.68(X_1 \times X_3) \\
 & - 1.25(X_2 \times X_3) + 0.74(X_2 \times X_4)
 \end{aligned} \quad (5)$$



## Production of biochar from the remaining biomass – closing the cycle of the biorefinery

After recovering the two most valuable compounds from pomegranate wastes, namely anthocyanins, ellagic acid, and its derivatives, an alternative biochar material was produced using the residual biomass usually discarded at the final extraction processes. The (D)ES composed of [Ch]Cl:OA (1 : 2) was selected considering two main factors: (i) acidic (D) ES can break down the complex structure of biomass, making it easier to convert into biochar.<sup>54</sup> Recent data showed the impact of this same (D)ES to disrupt a lignocellulosic matrix, more specifically in modifying kraft lignin.<sup>36</sup> Besides, (ii) carboxylic acids can also act as catalysts in biomass's thermal decomposition, showing several advantages to the process, namely by accelerating biochar production, optimizing energy consumption, and diminishing costs.<sup>55</sup> They help accelerate pyrolysis by promoting the breakdown of chemical bonds in the biomass, resulting in a more efficient conversion of waste into biochar. As happens with carboxylic acids, acidic (D)ES can also lower the thermal stability of the biomass components, allowing pyrolysis to occur at lower temperatures.<sup>56</sup> Based on Zhang's findings,<sup>35</sup> which demonstrated that using a DES composed of *p*-toluene sulfonic acid (*p*-TSA) and [Ch]Cl (1 : 1) to produce biochar from lignocellulosic-rich sources (namely hybrid poplar, Caribbean pine, and corn stalk) was an excellent strategy for achieving high yields, we opted to use the same operational conditions but with [Ch]Cl : OA. Oxalic acid in biochar production offers some advantages in terms of environmental impact, safety, and costs compared to *p*-TSA. Oxalic acid is more biodegradable and poses less risk to aquatic life and ecosystems compared to the higher toxicity associated with *p*-TSA. While both acids are corrosive, oxalic acid presents fewer severe health risks, making the working environment safer (see safety concerns, CAS-number: 144-62-7). In addition, oxalic acid is cheaper than *p*-TSA, which also needs to be considered. These benefits align with regulatory preferences that emphasize environmental safety, making oxalic acid a more favorable choice for biochar production.

In conventional methods, biochar yield varies depending on the procedure's temperature and the applied technique.<sup>57</sup> Usually, yields from 10% (>700 °C, by gasification approach) to 60% (<200 °C, hydrothermal carbonization)<sup>58</sup> are observed, highlighting that the (D)ES-mediated process developed here could be an easily feasible and high-performance alternative to produce biochar. In this work, a high-pressure cell was used as a vessel to transform the residual pomegranate wastes into biochar at a mild temperature (120 °C) and with low energy demands (magnetic stirring), which could also be used to produce biochar from different biomass sources in a more sustainable operating mode. In this study, the biochar production mediated by the (D)ES converted  $76 \pm 2\%$  of the residual biomass into biochar (yield, wt:wt), which is a significantly higher yield than those achieved using conventional systems (high-temperature pyrolysis with conventional reagents).

The morphology of the pomegranate biomass post-extraction and biochar is presented in Fig. 6. The pomegranate biomass presents a smooth surface (Fig. 6A), and the treatment that led to the biochar formation gave origin to carbon microparticles with a rough surface (Fig. 6B), resembling a charcoal structure, with a surface area of  $3.43 \text{ m}^2 \text{ g}^{-1}$ . Table S11 (ESI†) depicts the elemental composition of the biochar product, where the C, O, H, and N content was 43.96%, 47.90%, 5.48%, and 2.66%, respectively. The ratio between the atomic content of O and C (O/C) was 0.81, indicating a significant presence of oxygenated functional groups such as carboxyl, hydroxyl, and ether groups.<sup>27</sup> These groups can increase the reactivity of the biochar, enhancing its cation exchange capacity and interaction with nutrients and pollutants in the soil.<sup>59</sup> This makes this biochar a good candidate as an adsorbent material for pollutants and other chemical substances, such as synthetic dyes, as demonstrated in section 1 of the ESI.† Additionally, the atomic proportions of  $\text{H/C} = 1.49$  and  $(\text{N} + \text{O})/\text{C} = 0.86$  support this assessment. The low carbonization level of the produced biochar, as indicated by the H/C ratio, suggests a more aliphatic and less aromatic structure, which may result in a lower specific surface area and, thus, a reduced adsorption capacity.<sup>60</sup> However, the  $(\text{N} + \text{O})/\text{C}$  value indicates the presence of many oxygenated and

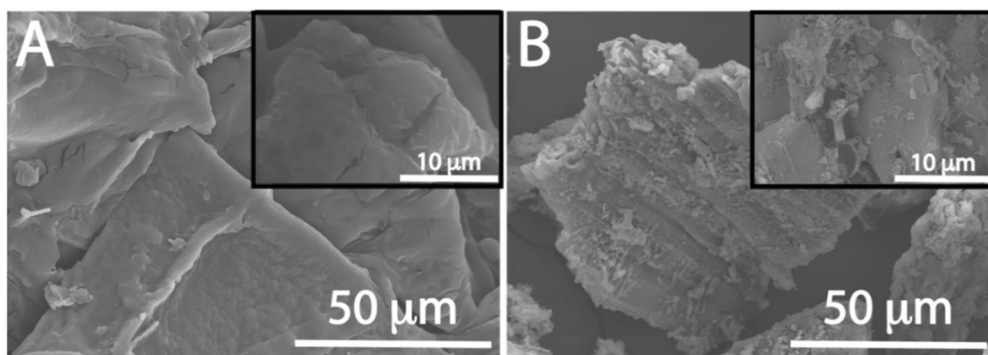


Fig. 6 Surface morphology of post-extraction pomegranate biomass (after recovering anthocyanins and ellagic acid-rich fractions) (A); biochar product – charcoal structure (B).



nitrogenated functional groups, such as carboxyl, hydroxyl, and amine groups. These functional groups can increase the biochar's reactivity and improve its ability to adsorb dyes through chemical interactions, such as hydrogen bonding and electrostatic interactions.<sup>28</sup> Oxygen- and nitrogen-containing functional groups can form specific interactions with the functional groups of synthetic dyes, enhancing adsorption.<sup>61</sup>

Additionally, the FTIR spectrum of biochar was compared with the FTIR spectrum of raw pomegranate (Fig. S7 – ESI†). The typical frequencies of pomegranate surface functional groups were identified (3292.68 cm<sup>-1</sup> for –NH and –OH of carboxylic acid, 2941 cm<sup>-1</sup> for aliphatic C–H, –CH<sub>3</sub> or –CH<sub>2</sub>, 1713.53 cm<sup>-1</sup> for carboxylic acid C=O, acetate, ketone, aldehyde, 1607.21 cm<sup>-1</sup> for C=C or C=N, deformation N–H of amines or amides, 1322.65/748.7 cm<sup>-1</sup> for aliphatic C–H, –CH<sub>3</sub> or –CH<sub>2</sub>, 1181.61 cm<sup>-1</sup> for the acid group (C=O), alcohols, phenols, ethers, and esters (C=C and C=N), and 1029.18/875.7 cm<sup>-1</sup> for C=S). However, an increase in the band's intensity at 1736 cm<sup>-1</sup> was observed, which could be associated with C=O stretching in ester groups formed by the esterification of oxalic acid molecules with hydroxyl groups from raw pomegranate. Fig. S8 (ESI†) shows that [Ch]:Cl:OA remains stable and only begins to decompose at temperatures above 180 °C. This supports the potential for recovering and reusing the DES in sequential biochar production cycles, contributing to a closed-loop system within the biorefinery, aligned with zero-waste principles. This observation is consistent with findings from Chen *et al.*,<sup>62</sup> who reported that the decomposition of oxalic acid is more accelerated between 180 °C and 230 °C. Beyond 230 °C, the degradation process becomes more pronounced.

### Design of an integrated multiproduct biorefinery from pomegranate wastes

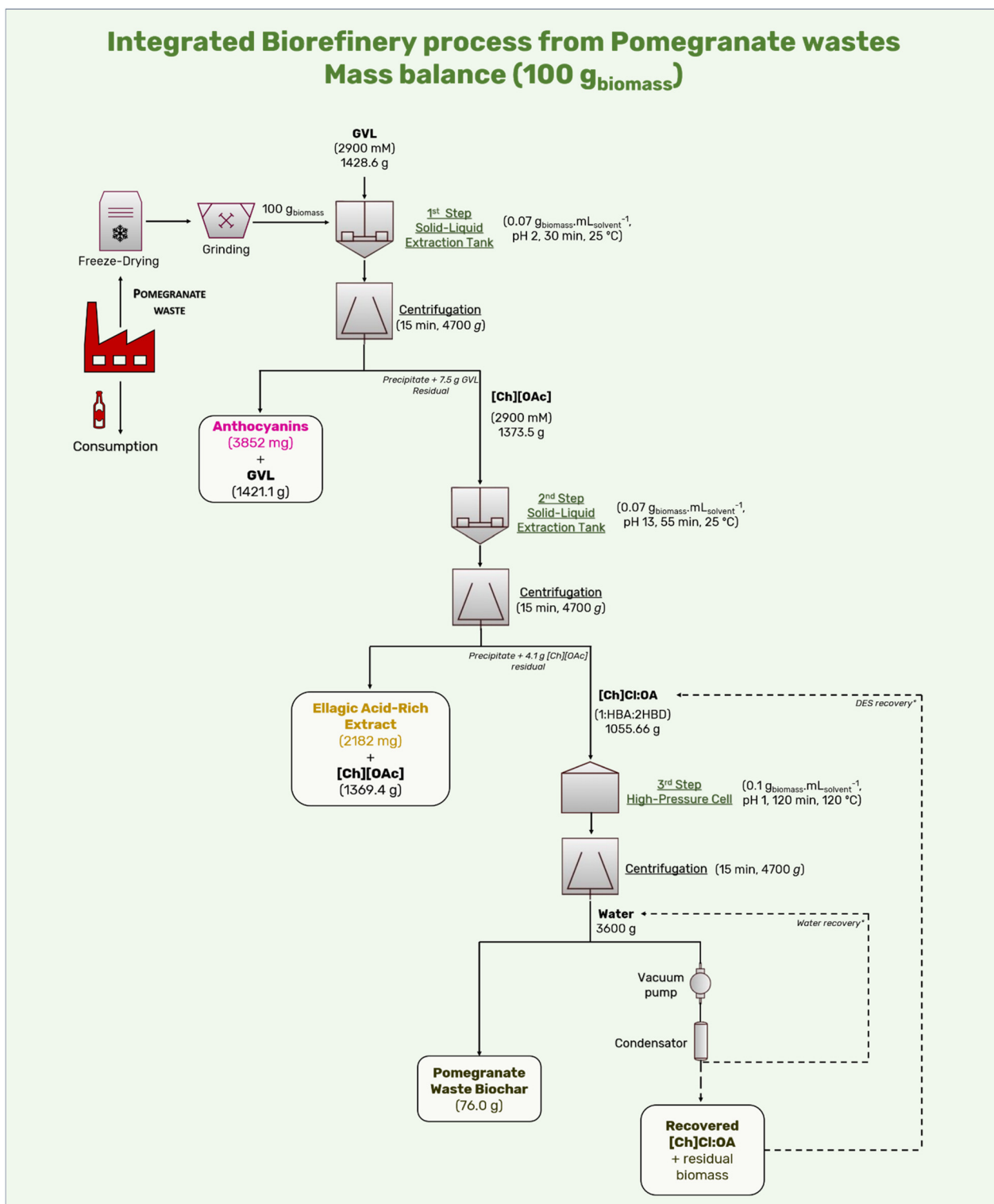
Fig. 7 illustrates the biorefinery process developed and the correspondent mass balance for lab scale, outlining the input of raw materials and solvents and the product output. As represented in Fig. 7, the first step was the pre-treatment of the pomegranate waste (freeze-drying + grinding), and after that, recovery of anthocyanins using an aqueous solution of GVL at 2.9 M, allowing an optimum extraction yield of  $38.52 \pm 0.06 \text{ mg}_{\text{anthocyanins}} \text{ g}_{\text{biomass}}^{-1}$ . The accumulation of GVL in the biomass residues obtained after the extraction of anthocyanins represents only 0.5% of the total added to the biorefinery process. GVL is a new sustainable green solvent,<sup>63</sup> and was shown to be an excellent alternative to replace conventional solvents used to extract anthocyanins, such as methanol (a low-performance solvent to recover pigments). Besides, since GVL is a chemically stable molecule (it does not suffer oxidation and degradation at room temperature and under pressure),<sup>8,63</sup> it could be considered a safe substance allowing better and safer storage and transportation.<sup>40,41</sup>

In the following step, the residual biomass after the extraction of anthocyanins was used to recover ellagic acid and derivatives using an aqueous solution of [Ch][OAc] at 2.9 M, enabling an optimum extraction recovery of  $21.82 \pm 0.36 \text{ mg}_{\text{ella-}}$

gic acid  $\text{g}_{\text{biomass}}^{-1}$ . The accumulation of [Ch][OAc] in the residue of biomass obtained after the extraction of ellagic acid represents only 0.3% of the total added to the biorefinery process. This system was fully optimized, which allowed us to obtain each pigment in its respective extraction media with a purity of at least 90%, confirming that GVL was an excellent solvent for selectively recovering anthocyanins. Finally, using a (D)ES, a mild-temperature alternative biochar production method was designed, producing a highly efficient adsorbent material that can be used in multiple applications, including water remediation of food and textile dyes (as proved in the present work and demonstrated in section 1 – ESI†). In the end, a zero-waste biorefinery was developed using pomegranate waste biomass.

### Green assessment of the developed process – Path2Green metric

The biorefinery developed here was evaluated using the Path2Green metric, a tool for assessing the sustainability of biomass valorization processes.<sup>37</sup> This evaluation is based on the 12 principles of green extraction, as detailed in Table S12 (ESI†), each one having the corresponding scores. The Path2Green metric offers a holistic overview to identify the extraction approach's strengths and potential red flags. The results calculated using the Path2Green mobile app are shown in Fig. 8, with the final process score prominently displayed in the center of the pictogram (Path2Green score: 0.401, a high positive score on a scale from –1.00 to +1.00). The pictogram displays icons corresponding to each of the 12 principles evaluated, where green coloration indicates good adherence, yellow indicates a neutral score, and red coloration indicates poor adherence to a principle, thus negatively impacting sustainability pillars. Among the 12 principles, principle 2 (preserving biomass integrity while minimizing transport's environmental impact) received a negative score (–1.00), the lowest possible. This low score is due to the high environmental impact of transporting biomass from its origin in California-USA (the biomass used in the lab scale), to Portugal, where the biorefinery platform was developed. Transporting the biomass from its origin to the extraction site indeed requires careful execution to prevent losses and contamination and ensure the extraction process's safety and quality. Additionally, it is crucial to consider the inherent environmental impact of transportation when evaluating each step.<sup>64</sup> In this context, it is obvious that it is not economically viable to implement this process on a large scale without considering the location. The optimal approach is to establish a biorefinery near water bodies and the biomass source site.<sup>65,66</sup> A second red flag is observed in principle 3, pre-treatment (optimization for pre-treatment avoidance and cost-effective techniques), which received a score of –0.20 due to physical pre-treatment techniques, specifically freeze-drying and grinding applied in the pomegranate residues before extraction. Physical pre-treatments are often preferred over chemical and biological methods for biomass preparation, particularly for extraction processes, due to their ease of implementation, lower environmental impact, and minimal use of additional chemicals.



**Fig. 7** Schematic representation of an integrated biorefinery process in lab scale and the respective mass balance (also in lab scale) based on an initial input of 100 g of pomegranate waste. The process is designed to fully utilize the biomass by recovering three key products: (I) anthocyanins using GVL (gamma-valerolactone), (II) an ellagic acid-rich fraction with [Ch][OAc] (cholinium acetate), and (III) biochar material produced from the remaining biomass after sequential extraction steps. Dashed lines indicate steps that were not experimentally optimized but are considered feasible. GVL: gamma-valerolactone, [Ch][OAc]: cholinium acetate, [Ch]Cl : OA: cholinium chloride : oxalic acid.



**Fig. 8** Pictogram illustrating the final score of the Path2Green metric, which is based on the 12 principles of green extraction. These principles are depicted around the pictogram in shades of green and red. Green means high adherence to the principle, while red indicates poor adherence.

These methods are generally simpler, more cost-effective, and require less complex infrastructure, making them an attractive option for industrial applications. However, at a large scale, freeze-drying imposes a high cost on the biorefinery. A recent techno-economic analysis of grape biorefineries highlighted the need for alternative drying techniques to mitigate these costs, especially considering freeze-drying on a large scale.<sup>67</sup> However, in cases where the biomass has high perishability, as is the case with the pomegranate waste used here, a pre-treatment of the biomass is essential to ensure the integrity and reproducibility of the compounds to be extracted. This step is crucial to prevent degradation and preserve the quality of the bioactive molecules, ensuring more efficient recovery during the extraction process.<sup>37</sup> A third concern is highlighted in principle 5 – scaling (ensuring reproducibility and a continuous extraction flow). The most readily scalable extraction techniques involve minimal procedural steps and operate within a continuous flow framework with *in situ* and automated systems.<sup>68</sup> Considering the fact that the lab scale biorefinery here developed was operating in batch regime with non-automated systems, and despite the fact that we cannot argue that it is straightforward to scale as a continuous flow process without testing it, we know from the unit operations included in the biorefinery that it can be scaled-up – at least to a semi-continuous process. In this context, a more sophisticated system is necessary to enhance the full scalability of the developed process. This includes automated unit operations (*e.g.* solvent feeding and solid–liquid extraction steps operating simultaneously) and adequate process simulation running to

have full control over the biorefinery platform.<sup>68</sup> A neutral score was assigned for principle 4 (minimize solvent usage, prioritizing those of biological origin and those that are biodegradable, and non-toxic). This principle takes into account both the handler safety and the potential environmental risks associated with the solvent, including its production process. In this study, a three-step biorefinery approach was developed to recover three valuable products from pomegranate waste: anthocyanins, an ellagic acid-rich fraction, and biochar material. The process employed three solvents: bio-based gamma-valerolactone (scoring 0.00 in the CHEM21 database,<sup>69</sup> which serves as a benchmark for solvent scoring in Path2Green), cholinium acetate (which can be synthesized as a bio-based IL but is mainly commercialized through synthetic routes, also scoring 0.00), and a eutectic solvent composed of cholinium chloride and oxalic acid. While these solvents present a more sustainable alternative to traditional volatile organic solvents derived from fossil fuels, there are still concerns regarding their production processes. Therefore, a neutral score (0.00) was applied in this metric to reflect these considerations. However, it is important to emphasize that selecting the appropriate solvent for biomass extraction platforms is a challenging task that requires balancing extraction efficiency and safety. In this process, we demonstrate the use of more sustainable options compared to traditional volatile organic solvents, such as methanol, which is commonly used to recover anthocyanins and ellagic acid derivatives. This is why we advocate for the development of bio-based solvent production pathways, particularly in the case of [Ch][OAc], where biological synthesis could offer a greener alternative to synthetic routes.

Despite the red flags associated with transport, pre-treatment, and scaling challenges, the other principles received positive scores. Using wasted pomegranate biomass (principle 1: selection of biomass that is naturally sourced or requires minimal resource usage for production) effectively adds value to usually neglected biomass. By extracting valuable compounds from the waste, especially food waste, we add value to what was considered refuse, allowing us to mitigate the environmental impact associated with its disposal, often conducted in environmentally detrimental ways,<sup>70</sup> thus benefiting the sustainability pillars environment, society, and economy. Considering the high energy demand to produce biochar by conventional pyrolysis reactions, a mild-temperature reaction using a non-volatile solvent is an intelligent strategy to reduce the carbon footprint compared to conventional methods.<sup>35</sup> The production of biochar from residual biomass post-extraction also supports a closed-loop biorefinery approach, aligning with principles 7 (maximizing the utilization and valorization of the biomass), 11 (repurposing: implementing closed-loop extraction systems using non-virgin materials), and 12 (waste management: minimizing waste and ensuring effective waste management). This comprehensive valorization of biomass using non-virgin raw materials and minimizing waste is the gold standard to be advocated.

Furthermore, the selective extraction of compounds using solvents that do not need to be removed from the final extracts

and produced with renewable energy aligns with principle 6 (purification: final application dictates the extent of purification), principle 8 (post-treatment: functionalizing natural products post-extraction to maximize benefits), and principle 9 (energy: prioritizing clean energy sources and high-efficiency extraction techniques), resulting in positive scores (+1.00). Finally, considering the broad range of applications for the obtained extracts (anthocyanins, ellagic acid and derivatives), the highest possible score (+1.00) was achieved for principle 10 (application: ensuring safety for applications in various domains). Anthocyanins can be applied in the pharmaceutical, cosmetic, nutraceutical, and spa product industries.<sup>71</sup> Similarly, ellagic acid and its derivatives, like anthocyanins, can also be used as preservatives and stabilizers,<sup>72,73</sup> while the biochar, as demonstrated in section 1 from the ESI,<sup>†</sup> was effective in the remediation of synthetic dyes in aqueous solutions, making it a potential filtering element for aqueous effluents. Therefore, the final Path2Green score for the developed biorefinery highlights strong adherence to sustainability principles and represents an equivalent carbon footprint of 288.50 gCO<sub>2</sub> g<sub>biomass</sub><sup>-1</sup>, calculated through the regression determined in the Path2Green original article.<sup>37</sup>

## Conclusion

In this study, a multiproduct biorefinery approach was developed to create a closed-loop pipeline for the valorization of pomegranate waste. Using green methods with non-conventional solvents, GVL optimized the extraction of anthocyanins, followed by the application of [Ch][OAc] responsible for the recovery of ellagic acid and derivatives from biomass residues. The target compounds obtained have several fields of applications, especially as colorant agents in food, besides being active ingredients in food, nutraceutical, and pharmaceutical products. The final residual biomass was converted into a highly efficient absorbent biochar using [Ch]Cl:OA and milder conditions. The biochar demonstrated excellent adsorption capacity for synthetic dyes, providing an effective strategy for aqueous effluent remediation. Finally, the “greenness” of the biorefinery process was analyzed through the 12 principles of green extraction and achieved a high Path2Green score of 0.401, confirming its sustainability and efficiency. The developed approach represents a significant advancement in sustainable biorefinery technologies, highlighting its potential for reducing waste, minimizing environmental impact, and promoting the use of bio-based solvents in industrial applications. Additionally, the study emphasizes the critical role of alternative solvents in sustainable extraction processes, providing new perspectives for experts on the potential of bio-based and non-conventional solvents in industrial applications. By exploring these alternatives, this research fosters innovation in green chemistry and encourages the development of environmentally friendly practices that can replace harmful solvents traditionally used in extraction. This discussion not only broadens the scope of sustainable solvent use, but also con-

tributes to advancing cleaner, more responsible production methods across various sectors.

## Data availability

The data prepared to develop this article are included in the manuscript and ESI.<sup>†</sup>

## Conflicts of interest

There are no conflicts to declare.

## Acknowledgements

This work was supported by “Fundação de Amparo à Pesquisa do Estado de São Paulo – FAPESP” through the projects (2018/14582-5 and 2019/13496-0) and fellowships (L. M. de S. M.: 2020/08421-9, 2021/11022-1; L. S. C.: 2020/03623-2, 2021/11023-8). This work was supported by the Conselho Nacional de Desenvolvimento Científico e Tecnológico (CNPq, Brazil) (productivity grant: 302610/2021-9). This work was developed within the scope of the project CICECO-Aveiro Institute of Materials (UIDB/50011/2020 (DOI: [10.54499/UIDB/50011/2020](https://doi.org/10.54499/UIDB/50011/2020)), UIDP/50011/2020 (DOI: [10.54499/UIDP/50011/2020](https://doi.org/10.54499/UIDP/50011/2020)) and LA/P/0006/2020 (DOI: [10.54499/LA/P/0006/2020](https://doi.org/10.54499/LA/P/0006/2020))), financed by national funds through the FCT/MECTES (PIDDAC). V. S. acknowledges Cost Action CA19118 – EsSENce. The authors are also grateful to the FCT for the doctoral grants of B. M. C. V. (2022.13816.BD). F. H. B. S. acknowledges FCT – Fundação para a Ciência e a Tecnologia, I.P. for the researcher contract CEECIND/07209/2022 under the Scientific Employment Stimulus – Individual Call 2022.

## References

- 1 Y. K. Dwivedi, L. Hughes, A. K. Kar, A. M. Baabdullah, P. Grover, R. Abbas, D. Andreini, I. Abumoghli, Y. Barlette, D. Bunker, L. Chandra Kruse, I. Constantiou, R. M. Davison, R. De', R. Dubey, H. Fenby-Taylor, B. Gupta, W. He, M. Kodama, M. Mäntymäki, B. Metri, K. Michael, J. Olaisen, N. Panteli, S. Pekkola, R. Nishant, R. Raman, N. P. Rana, F. Rowe, S. Sarker, B. Scholtz, M. Sein, J. D. Shah, T. S. H. Teo, M. K. Tiwari, M. T. Vendelø and M. Wade, *Int. J. Inf. Manage.*, 2022, **63**, 102456.
- 2 United Nations, Sustainable Development Goals, <https://www.un.org/sustainabledevelopment/sustainable-development-goals/>, (accessed 8 January 2023).
- 3 J. H. Clark, *Green Chem.*, 2019, **21**, 1168–1170.
- 4 H. A. Ruiz, W. G. Sganzerla, V. Larnaudie, R. J. Veersma, G. van Erven, Shiva, L. J. Ríos-González, R. M. Rodríguez-Jasso, G. Rosero-Chasoy, M. D. Ferrari, M. A. Kabel, T. Forster-Carneiro and C. Lareo, *Bioresour. Technol.*, 2023, **369**, 128469.



- 5 H. Y. Leong, C.-K. Chang, K. S. Khoo, K. W. Chew, S. R. Chia, J. W. Lim, J.-S. Chang and P. L. Show, *Biotechnol. Biofuels*, 2021, **14**, 87.
- 6 F. G. Calvo-Flores and F. J. Martin-Martinez, *Front. Chem.*, 2022, **10**, DOI: [10.3389/fchem.2022.973417](https://doi.org/10.3389/fchem.2022.973417).
- 7 F. G. Calvo-Flores, M. J. Monteagudo-Arrebola, J. A. Dobado and J. Isac-García, *Top. Curr. Chem.*, 2018, **376**, 18.
- 8 M. Kholany, I. P. E. Macário, T. Veloso, L. S. Contieri, B. M. C. Vaz, J. L. Pereira, C. Nunes, J. A. P. Coutinho, M. A. Rostagno, S. P. M. Ventura and L. M. de Souza Mesquita, *Green Chem.*, 2024, **26**(5), 2793–2806.
- 9 S. P. M. Ventura, F. A. e Silva, M. V. Quental, D. Mondal, M. G. Freire and J. A. P. Coutinho, *Chem. Rev.*, 2017, **117**, 6984–7052.
- 10 A. P. Abbott, D. Boothby, G. Capper, D. L. Davies and R. K. Rasheed, *J. Am. Chem. Soc.*, 2004, **126**, 9142–9147.
- 11 J. Flieger and M. Flieger, *Int. J. Mol. Sci.*, 2020, **21**, 6267.
- 12 I. P. E. Macário, S. P. M. Ventura, J. L. Pereira, A. M. M. Gonçalves, J. A. P. Coutinho and F. J. M. Gonçalves, *Ecotoxicol. Environ. Saf.*, 2018, **165**, 597–602.
- 13 D. C. Murador, L. M. de Souza Mesquita, N. Vannuchi, A. R. C. Braga and V. V. de Rosso, *Curr. Opin. Food Sci.*, 2019, **26**, 25–34.
- 14 F. S. Bragagnolo, M. M. Strieder, R. S. Pizani, L. M. de Souza Mesquita, M. González-Miquel and M. A. Rostagno, *TrAC, Trends Anal. Chem.*, 2024, **175**, 117726.
- 15 B. Tsegaye, S. Jaiswal and A. K. Jaiswal, *Foods*, 2021, **10**, 1174.
- 16 I. Ismail Iid, S. Kumar, S. Shukla, V. Kumar and R. Sharma, *Trends Food Sci. Technol.*, 2020, **97**, 317–340.
- 17 Q. Xiang, M. Li, J. Wen, F. Ren, Z. Yang, X. Jiang and Y. Chen, *J. Food Biochem.*, 2022, **46**, e14105.
- 18 K. Ko, Y. Dadmohammadi and A. Abbaspourrad, *Foods*, 2021, **10**, 657.
- 19 B. Singh, J. P. Singh, A. Kaur and N. Singh, *Food Chem.*, 2018, **261**, 75–86.
- 20 R. Meccariello and S. D'Angelo, *Antioxidants*, 2021, **10**, 507.
- 21 L. M. de Souza Mesquita, M. Martins, L. P. Pisani, S. P. M. Ventura and V. V. de Rosso, *Compr. Rev. Food Sci. Food Saf.*, 2021, **20**, 787–818.
- 22 N. Goyal and F. Jerold, *Environ. Sci. Pollut. Res.*, 2021, **30**(10), 25148–25169.
- 23 S. Dey and B. H. Nagababu, *Food Chem. Adv.*, 2022, **1**, 100019.
- 24 C. Ramos-Souza, D. H. Bandoni, A. P. A. Bragotto and V. V. De Rosso, *Compr. Rev. Food Sci. Food Saf.*, 2023, **22**, 380–407.
- 25 European Commission, Communication from the commission to the European parliament, the council, the European economic and social committee and the committee of the regions – A New Circular Economy Action Plan For a Cleaner and more competitive Europe, <https://eur-lex.europa.eu/legal-content/EN/TXT/?qid=1583933814386%7B%5C%7Duri=COM:2020:98:FIN>, (accessed 8 January 2023).
- 26 P. Srivatsav, B. S. Bhargav, V. Shanmugasundaram, J. Arun, K. P. Gopinath and A. Bhatnagar, *Water*, 2020, **12**, 3561.
- 27 M. Ilić, F.-H. Haegel, A. Lolić, Z. Nedić, T. Tosti, I. S. Ignjatović, A. Linden, N. D. Jablonowski and H. Hartmann, *PLoS One*, 2022, **17**, e0277365.
- 28 X.-F. Tan, S.-S. Zhu, R.-P. Wang, Y.-D. Chen, P.-L. Show, F.-F. Zhang and S.-H. Ho, *Chin. Chem. Lett.*, 2021, **32**, 2939–2946.
- 29 X. Yang, S. Zhang, M. Ju and L. Liu, *Appl. Sci.*, 2019, **9**, 1365.
- 30 F. Eckert and A. Klamt, *AIChE J.*, 2002, **48**, 369–385.
- 31 Y. Marcus, *Chem. Soc. Rev.*, 1993, **22**, 409.
- 32 M. M. Giusti and R. E. Wrolstad, in *Handbook of Food Analytical Chemistry*, John Wiley & Sons, Inc., Hoboken, NJ, USA, 2005, pp. 5–69.
- 33 L. M. de Souza Mesquita, L. S. Contieri, V. L. Sanches, R. Kamikawachi, F. H. B. Sosa, W. Vilegas and M. A. Rostagno, *Food Chem.*, 2023, **428**, 136814.
- 34 L. De Souza Mesquita, C. Caria, P. Santos, C. Ruy, N. Da Silva Lima, D. Moreira, C. Da Rocha, D. Murador, V. De Rosso, A. Gambero and W. Vilegas, *Molecules*, 2018, **23**, 2114.
- 35 Y. Zhang, Y. Meng, L. Ma, H. Ji, X. Lu, Z. Pang and C. Dong, *J. Cleaner Prod.*, 2021, **324**, 129270.
- 36 F. H. B. Sosa, D. O. Abranches, A. M. da Costa Lopes, J. A. P. Coutinho and M. C. da Costa, *ACS Sustainable Chem. Eng.*, 2020, **8**, 18577–18589.
- 37 L. M. de Souza Mesquita, L. S. Contieri, F. A. e Silva, R. H. Bagini, F. S. Bragagnolo, M. M. Strieder, F. H. B. Sosa, N. Schaeffer, M. G. Freire, S. P. M. Ventura, J. A. P. Coutinho and M. A. Rostagno, *Green Chem.*, 2024, **26**(19), 10087–10106.
- 38 V. Caballero, M. Estévez, F. A. Tomás-Barberán, D. Morcuende, I. Martín and J. Delgado, *J. Agric. Food Chem.*, 2022, **70**, 16273–16285.
- 39 T. Brouwer and B. Schuur, *Ind. Eng. Chem. Res.*, 2019, **58**, 8903–8914.
- 40 F. Kerkel, M. Markiewicz, S. Stolte, E. Müller and W. Kunz, *Green Chem.*, 2021, **23**, 2962–2976.
- 41 D. M. Alonso, S. G. Wettstein and J. A. Dumesic, *Green Chem.*, 2013, **15**, 584.
- 42 F. Chemat, M. A. Vian and G. Cravotto, *Int. J. Mol. Sci.*, 2012, **13**, 8615–8627.
- 43 C. Polesca, H. Passos, B. M. Neves, J. A. P. Coutinho and M. G. Freire, *Green Chem.*, 2023, **25**, 1424–1434.
- 44 R. Santiago, I. Díaz, M. González-Miquel, P. Navarro and J. Palomar, *Fluid Phase Equilib.*, 2022, **560**, 113495.
- 45 Y. Q. Goh, G. Cheam and Y. Wang, *J. Agric. Food Chem.*, 2021, **69**, 10774–10789.
- 46 J. Queffelec, W. Beraud, M. Dolores Torres and H. Domínguez, *Sustainable Chem. Pharm.*, 2024, **38**, 101478.
- 47 M. Kholany, I. P. E. Macário, T. Veloso, L. S. Contieri, B. M. C. Vaz, J. L. Pereira, C. Nunes, J. A. P. Coutinho, M. A. Rostagno, S. P. M. Ventura and L. M. de Souza Mesquita, *Green Chem.*, 2024, **26**, 2793–2806.

- 48 S. S. Silva, M. Justi, J.-B. Chagnoleau, N. Papaiconomou, X. Fernandez, S. A. O. Santos, H. Passos, A. M. Ferreira and J. A. P. Coutinho, *Sep. Purif. Technol.*, 2023, **304**, 122344.
- 49 N. I. Haykir and J. Viell, *Ind. Eng. Chem. Res.*, 2024, **63**, 12251–12264.
- 50 I. P. E. Macário, T. Veloso, J. L. Pereira, S. P. M. Ventura and J. A. P. Coutinho, in *Encyclopedia of Ionic Liquids*, Springer Singapore, Singapore, 2020, pp. 1–17.
- 51 M. Zakrewsky, A. Banerjee, S. Apte, T. L. Kern, M. R. Jones, R. E. Del Sesto, A. T. Koppisch, D. T. Fox and S. Mitragotri, *Adv. Healthcare Mater.*, 2016, **5**, 1282–1289.
- 52 J. M. Gomes, S. S. Silva and R. L. Reis, *Chem. Soc. Rev.*, 2019, **48**, 4317–4335.
- 53 K. S. Egorova, E. G. Gordeev and V. P. Ananikov, *Chem. Rev.*, 2017, **117**, 7132–7189.
- 54 F. Amalina, A. S. A. Razak, S. Krishnan, A. W. Zularisam and M. Nasrullah, *Cleaner Mater.*, 2022, **3**, 100045.
- 55 C. Larabi, W. al Maksoud, K. C. Szeto, A. Roubaud, P. Castelli, C. C. Santini and J. J. Walter, *Bioresour. Technol.*, 2013, **148**, 255–260.
- 56 M. Pahnla, A. Koskela, P. Sulasalmi and T. Fabritius, *Energies*, 2023, **16**, 6936.
- 57 P. R. Yaashikaa, P. S. Kumar, S. Varjani and A. Saravanan, *Biotechnol. Rep.*, 2020, **28**, e00570.
- 58 S. Praveen, J. Jegan, T. Bhagavathi Pushpa, R. Gokulan and L. Bulgariu, *Biochar*, 2022, **4**, 10.
- 59 S. Adhikari, E. Moon and W. Timms, *J. Cleaner Prod.*, 2024, **446**, 141454.
- 60 S. Wijitkosum and P. Jiwnok, *Appl. Sci.*, 2019, **9**, 3980.
- 61 T. G. Ambaye, M. Vaccari, E. D. van Hullebusch, A. Amrane and S. Rtimi, *Int. J. Environ. Sci. Technol.*, 2021, **18**, 3273–3294.
- 62 K. Chen, Y. Li, C. Zhang, S. Zhou, J. Li, P. Li, Z. Sun, B. Meng and D. Fu, *IOP Conf. Ser. Earth Environ. Sci.*, 2020, **600**, 012003.
- 63 I. T. Horváth, H. Mehdi, V. Fábos, L. Boda and L. T. Mika, *Green Chem.*, 2008, **10**, 238–242.
- 64 S. M. Zahraee, S. R. Golroudbary, N. Shiwakoti, P. Stasinopoulos and A. Kraslawski, *Procedia CIRP*, 2021, **100**, 780–785.
- 65 C. Ong, G. Deprés, J. Hollebecq, M. O. Shaiffudin Hishamudin, N. Kamaruddin, A. R. Anugerah, A. N. Amir Mustafa and J. Roda, *GCB Bioenergy*, 2020, **12**, 910–922.
- 66 A. Serrano, J. Faulin, P. Astiz, M. Sánchez and J. Belloso, *Transp. Res. Procedia*, 2015, **10**, 704–713.
- 67 L. M. de Souza Mesquita, J. Viganó, P. Veggi, L. S. Contieri, F. H. B. Sosa, V. Vera de Rosso, S. P. M. Ventura and M. A. Rostagno, *Sep. Purif. Technol.*, 2024, **347**, 127647.
- 68 M. T. Tudesco, E. G. Moschetta and E. A. Voight, *Org. Process Res. Dev.*, 2018, **22**, 1564–1569.
- 69 D. Prat, A. Wells, J. Hayler, H. Sneddon, C. R. McElroy, S. Abou-Shehadeh and P. J. Dunn, *Green Chem.*, 2016, **18**, 288–296.
- 70 Y. Wang, M. Su, L. Shen and R. Tang, *J. Cleaner Prod.*, 2021, **284**, 125373.
- 71 T. Belwal, G. Singh, P. Jeandet, A. Pandey, L. Giri, S. Ramola, I. D. Bhatt, P. R. Venskutonis, M. I. Georgiev, C. Clément and Z. Luo, *Biotechnol. Adv.*, 2020, **43**, 107600.
- 72 J. Sharifi-Rad, C. Quispe, C. M. S. Castillo, R. Caroca, M. A. Lazo-Vélez, H. Antonyak, A. Polishchuk, R. Lysiuk, P. Oliinyk, L. De Masi, P. Bontempo, M. Martorell, S. D. Daştan, D. Rigano, M. Wink and W. C. Cho, *Oxid. Med. Cell. Longevity*, 2022, **2022**, 1–24.
- 73 F. Zhou, T. Peterson, Z. Fan and S. Wang, *Nutrients*, 2023, **15**, 3881.